ISSN: 2277-9655
(I2OR), Publication Impact Factor: 3.785

IJESRT

INTERNATIONAL JOURNAL OF ENGINEERING SCIENCES & RESEARCH TECHNOLOGY

EFFECT OF THERMOPHORESIS ON MIXED CONVECTION FLOW OF A ROTATING FLUID OVER A ROTATING CONE IN A NON-DARCY POROUS MEDIUM

S.Hariprasad Raju*, B.Mallikarjuna[*], S.V.K.Varma and K.Janardhan
Department of Mathematics, Sri Venkateswara University, Tirupati, India.
[*]Department of Mathematics, BMS College of Engineering, Bangalore, India.
Department of Mathematics, Santhiram Engineering College, Nandyal, India.

ABSTRACT

A Numerical analysis is performed to study the effect of Thermophoresis on steady mixed convective boundary layer flow of a rotating fluid over a rotating vertical cone in a non-Darcy porous medium. The governing boundary layer equations are formulated and numerical results are obtained by employing shooting technique. The present numerical solutions are compared with earlier existing results and good agreement has been obtained between existing results. Numerical results for fluid flow characteristics, fluid velocities (tangential, circumferential and normal), temperature and concentration distributions as well as tangential and circumferential skin friction coefficients, Nusselt number and Sherwood number are presented graphically and discussed for different values of physical parameters such as inverse Darcy parameter, Forchheimer parameter, ratio of angular velocities, relative temperature parameter and thermophoretic coefficient. Increasing Forchheimer parameter retards tangential skin friction coefficient, Nusselt number and Sherwood number but enhances circumferential skin friction coefficient. As increase in ratio of angular velocities tangential and circumferential skin friction coefficients are increased but Nusselt number and Sherwood number results are reduced. The wall thermophoretic velocity profile increases with increasing values of Forchheimer parameter and ratio of angular velocities and with decreasing values of relative temperature parameter.

KEYWORDS: Thermophoresis, Non-Darcy, Rotating Fluid, Rotating Cone.

INTRODUCTION

Coupled heat and mass transfer by mixed convection in a fluid saturated porous medium received considerable interest during last several decades. This is mainly because of the enormous applications of fluid flow on heat and mass transfer through porous medium, such as storage of radioactive nuclear waste, separation processes in chemical industries, fiber insulation, filtration, the migration of moisture in fibrous insulation, transport processes in aquifers, groundwater pollution, geothermal extraction, transpiration cooling, the extraction of geothermal energy, underground disposal of nuclear waste, and the spreading of chemical pollutants in saturated soil, etc.,. It has been noticed that Darcy law is valid for low-velocity flows or where the Reynolds number based on the volume-averaged velocity and pore length scale is less than O(1) [1]. However for a high-speed flow the non-Darcy law is found to be more accurate and appropriate. Theoretical and experimental work of thermal and solutal convection in porous media, with special emphasis on industrial applications are presented in the recent books by Nield and Bejan [1], Ingham and Pop [2], Vafai [3], and Bejan et al. [4].

Free and forced convective flow of heat and mass transfer in a rotating system is considerable interest in various industrial, technological and engineering applications such as in the design of turbo machines and turbines. Das [5] studied the influence of thermal radiation and first ordered chemical reaction on MHD free convective flow of a micropolar fluid over a semi-infinite vertical porous plate in a fluid saturated porous medium. Schuler et.al [6] investigated numerical predictions of the effect of rotation on fluid flow and heat transfer in an engine similar two pass internal cooling channel with smooth and ribbed walls. Rashidi et.al [7] studied the effect of second law of thermodynamic on steady MHD convective boundary layer flow due to a rotating porous disk in a nanofluid. Bhuvanavijaya and Mallikarjuna [8] investigated temperature dependent thermal conductivity and variable porosity regime on convective heat and mass transfer flow over vertical plate in a rotating system. Satyanarayana et.al [9]

ISSN: 2277-9655
(I2OR), Publication Impact Factor: 3.785
(ISRA), Journal Impact Factor: 2.114

studied heat source effects on heat and mass transfer flow of a MHD Nanofluid over a vertical plate in a rotating system with porous medium with thermal radiation.
The mixed convective heat and mass transfer over a rotating vertical cone embedded in a fluid saturated porous medium is an important phenomenon for spin stabilized missiles, geothermal reservoirs, rotating heat exchanger and containers of nuclear waste disposal. Saravanan [10] investigated theoretically on the onset of convection induced by centrifugal acceleration in a MHD fluid filled porous medium. Chamkha and Ahmed [11] studied unsteady MHD effect on heat and mass transfer by mixed convection flow in the forward stagnation region of a rotating sphere at different wall conditions. Nadeem and Saleem [12] investigated unsteady mixed convection flow of a rotating second grade nanofluid in a rotating cone. Hariprasad et.al [13] studied thermophoretic effect on convective heat and mass transfer flow over a rotating vertical cone in a porous medium with chemical reaction.

In this investigation, it was proposed to study the effect of thermophoretic on double diffusive convective flow of boundary layer rotating fluid over a non-Darcy porous medium. Numerical solutions of the boundary layer governing equations are obtained and discussion is presented for different values of the thermophoresis coefficient, ratio of angular velocities, Forchhiemer parameter governing the problem. The dependency of skin friction coefficients, local rate of heat and mass transfer on these parameters are discussed. To the best of my knowledge this study is not appeared in the scientific literature.

FORMULATION OF THE PROBLEM

We consider the steady, laminar, axisymmetric, incompressible viscous fluid over a rotating vertical cone in a fluid saturated porous medium. Physical configuration and coordinate of the system is given in fig. 1. The rotating cone is assumed to be variable temperature and variable concentration, higher than ambient fluid temperature and concentration. We consider the rectangular curvilinear coordinate system. The fluid saturated porous medium is assumed to be homogeneous and isotropic which is in locally thermodynamic equilibrium with solid matrix. The fluid and porous medium properties are assumed to be constant except density in the buoyancy force term. The buoyancy force is made up of two components; the fluid temperature and concentration variations. In addition, the porous medium is modeled using well-known and validated Forchheimer drag model. This incorporates a linear Darcian drag for low velocity fluids and a second order resistance for high velocity flow. The governing boundary layer equations for flow, heat and mass transfer near the rotating vertical cone can be written as

$$\frac{\partial(xu)}{\partial x}+\frac{\partial(xw)}{\partial z}=0 \tag{1}$$

$$u\frac{\partial u}{\partial x}+w\frac{\partial u}{\partial z}-\frac{v^2}{x}=-\frac{v_e^2}{x}+\nu\frac{\partial^2 u}{\partial z^2}-\frac{\nu}{K}u-\frac{C_b}{\rho}u^2+g\beta_T\left(T-T_\infty\right)\cos(\alpha)+g\beta_c\left(C-C_\infty\right)\cos(\alpha) \tag{2}$$

$$u\frac{\partial v}{\partial x}+w\frac{\partial v}{\partial z}+\frac{uv}{x}=\nu\frac{\partial^2 v}{\partial z^2}-\frac{\nu}{K}v-\frac{C_b}{\rho}v^2 \tag{3}$$

$$\left(u\frac{\partial T}{\partial x}+w\frac{\partial T}{\partial z}\right)=\frac{k_e}{\rho c_p}\frac{\partial^2 T}{\partial z^2} \tag{4}$$

$$u\frac{\partial C}{\partial x}+w\frac{\partial C}{\partial z}+\frac{\partial}{\partial z}\left(Cv_t\right)=D\frac{\partial^2 C}{\partial z^2} \tag{5}$$

The corresponding boundary conditions are

$$\begin{aligned} &u=0, v=r\Omega_1, w=0, T=T_w(x),\ C=C_w(x) \quad at\ \ z=0\\ &u=0, v=0, T=T_\infty, C=C_\infty \qquad\qquad as\ \ z\to\infty \end{aligned} \tag{6}$$

where u, v and w are the velocity components along the tangential (x), circumferential or azimuthal (y) and normal (z) directions respectively, r is the radius of the cone, Ω_1 and Ω_2 are the angular velocities of the cone and fluid respectively, ρ is the fluid density, μ is the dynamic viscosity, c_p is the specific heat at constant pressure, C_b is

ISSN: 2277-9655
(I2OR), Publication Impact Factor: 3.785
(ISRA), Journal Impact Factor: 2.114

the inertial coefficient, g is the acceleration due to gravity. Also α represents the cone apex half angle, K is the permeability of the porous medium, k_e is the effective thermal conductivity and D is the molecular diffusivity.

NON-DIMENALISATION

Now we introduce the following non-dimensional variables to get the non-dimensional governing equations

$$\eta = \left(\frac{\Omega \sin(\alpha)}{\nu}\right)^{1/2} z, \quad u = x\Omega\sin(\alpha)F(\eta), v = x\Omega\sin(\alpha)G(\eta), \quad r = x\sin(\alpha)$$

$$w = \left(\nu\Omega\sin(\alpha)\right)^{1/2} H(\eta), \quad \theta(\eta) = \frac{T - T_\infty}{T_w - T_\infty}, \quad \phi(\eta) = \frac{C - C_\infty}{C_w - C_\infty} \tag{7}$$

$$T_w(x) - T_\infty = \frac{(T_L - T_\infty)x}{L}, \quad C_w(x) - C_\infty = \frac{(C_L - C_\infty)x}{L}$$

where L being the cone slant height and T_L being the cone surface temperature and C_L being the cone surface concentration at the base(x=L).

Using equation (7), the equations (1) – (6) are transformed into non-dimensional boundary layer equation as follows

$$F = -\frac{1}{2}H' \tag{8}$$

$$H''' - HH'' - Da^{-1}H + \frac{1}{2}H'^2(1+\Gamma) - 2\left(G^2 - (1-\lambda)^2\right) - 2g_s(\theta + N\phi) = 0 \tag{9}$$

$$G'' - HG' + H'G - \Gamma G^2 - Da^{-1}G = 0 \tag{10}$$

$$\theta'' - \Pr\left(H\theta' - \frac{1}{2}H'\theta\right) = 0 \tag{11}$$

$$\phi'' + Sc\left(\frac{1}{2}H'\phi - H\phi'\right) + \frac{ScNt}{\theta N_t + 1}\left(\phi'\theta' + \phi\theta'' - \frac{Nt\phi\theta'^2}{\theta Nt + 1}\right) = 0 \tag{12}$$

Boundary conditions

$$\begin{aligned} &H = 0, \quad H' = 0, \quad G = \lambda, \quad \theta = 1, \quad \phi = 1 \quad && at\ \eta = 0 \\ &H' = 0, \quad G = 1 - \lambda, \quad \theta = 0, \quad \phi = 0 && as\ \eta \to \infty \end{aligned} \tag{13}$$

Where $Da^{-1} = \frac{\nu}{K\Omega\sin\alpha}$ is the inverse of Darcy number, $\Gamma = \frac{C_b L}{\rho}$ is the Dimensionless porous medium, $Gr = \frac{g\beta_T(T_\omega - T_\infty)L^3\cos\alpha}{\nu^2}$ is the Grashof number, $N = \frac{\beta_C(C_w - C_\infty)}{\beta_T(T_w - T_\infty)}$ is the buoyancy ratio, $\mathrm{Re} = \frac{\Omega L^2 \sin\alpha}{\nu}$ is the local Reynolds number, $g_s = \frac{Gr}{\mathrm{Re}^2}$ is the mixed convection parameter, $\Pr = \frac{\mu c_p}{\rho}$ is the Prandtl number, $Sc = \frac{\nu}{D}$ is the Schmidt number, $Nt = \frac{T_w - T\infty}{T_\infty}$ is the relative thermophoretic temperature parameter, Ω_1 is the angular velocities of the cone, Ω_2 is the angular velocities of the free stream fluid, $\lambda = \frac{\Omega_1}{\Omega}$ is the ratio of angular velocity of the cone to the composite angular velocity.

ISSN: 2277-9655
(I2OR), Publication Impact Factor: 3.785
(ISRA), Journal Impact Factor: 2.114

The engineering design quantities of important physical interest include the skin friction coefficients in x (tangential) and y (azimuthal) directions, local Nusselt number and local Sherwood number, which are given in non-dimensional form.

$$\mathrm{Re}^{1/2} C_{fx} = -H''(0) \tag{14}$$

$$2^{-1}\mathrm{Re}^{1/2} C_{fy} = -G'(0) \tag{15}$$

$$\mathrm{Re}^{-1/2} Nu_x = -\theta'(0) \tag{16}$$

$$\mathrm{Re}^{-1/2} Sh_x = -\phi'(0) \tag{17}$$

NUMERICAL METHOD OF SOLUTION

A set of governing boundary layer non linear coupled equations (8) – (12) with boundary conditions (13) for flow, energy and concentration are solved by using shooting technique that uses Runge-kutta method and Newton-Raphson method (See Srinivasacharya et.al [14] and Hariprasad et.al [13]).

In order to verify the accuracy of the present applied numerical method, particular results are compared with those available in the literature. A comparison of tangential and circumferential skin friction coefficients and Nusselt number for the presents results with those reported earlier by Himasekhar et.al [15] in the absence of current mass transfer rotating fluid, and the absence of the effects of thermophoresis, inverse Darcy parameter and Forchheimer parameters is done and shown in Table-1. From these tables values it can be seen that good agreement between the present and earlier published results. This lends confidence in the numerical results reported in this work.

Figure:

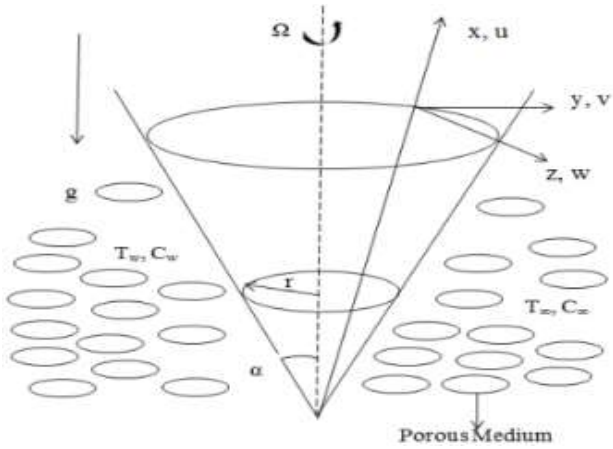

Fig 1: Physical configuration and co-ordinate system

RESULTS AND DISCUSSION

In this study, representative numerical results are reported with the help of graphical representations. Numerical results were obtained for different values of pertinent parameters such as Forchheimer parameter (Γ) ratio of angular velocities (λ), relative temperature difference parameter (Nt) and Thermophoresis coefficient (k). Figures 2 - 6 represent the variation of Forchheimer parameter on tangential, circumferential and normal velocity, temperature and concentration profiles respectively. From fig. 2 it is observed that increasing in Γ results deceleration near the cone surface until it reaches a particular value and then enhances until reaches the constant, at the outside of the boundary layer. From fig. 3 it is seen that circumferential velocity profile increases near the boundary up to reaching certain value and then decreases until becomes constant at the outside of the boundary layer with increasing values of Forchheimer parameter. From fig 4-6, it is noticed that increasing Forchheimer parameter

ISSN: 2277-9655
(I2OR), Publication Impact Factor: 3.785
(ISRA), Journal Impact Factor: 2.114

enhances normal velocity, temperature and concentration profiles. Thus, increase in Forchheimer parameter leads to enhance hydrodynamic, thermal and solutal boundary layer thickness.

The variation of ratio of angular velocities λ on tangential, circumferential and normal velocity, temperature and concentration profiles is represented in figures 7-11 respectively. The value $\lambda = 0$ represents the fluid is rotating and cone is at rest while the fluid and cone are rotating with same angular velocities in the same direction for $\lambda = 0.5$. Fig. 7 reveals that tangential velocity profile decreases considerably with increase in λ for both cases of $\lambda > 0.5$ and $\lambda < 0.5$. From fig. 8 it is reported that the variation of ratio angular velocity results reported similar results with those of Forchheimer parameter on circumferential velocity profile as shown in fig. 3. But Circumferential velocity profile is more pronounced for larger values of λ. From fig. 9 -11, it is seen that increase in ratio of angular velocities tends to enhance normal velocity, temperature and concentration profiles. In other words the thickness of hydrodynamic, thermal and solutal boundary layer is accelerated with increase in λ. Less variation in temperature and concentration profiles is noticed in figures 10 and 11, due to increase in ratio of angular velocities.

The effect of relative temperature parameter (Nt) inverse Darcy parameter $\left(Da^{-1}\right)$ and thermophoretic coefficient (k) on tangential and circumferential skin friction coefficients, Nusselt number and Sherwood numbers is exhibited in figures 12-15 respectively. It is observed from these figures that increasing relative temperature parameter (Nt) accelerates tangential and circumferential skin friction coefficients and Nusselt number while decelerates Sherwood number. It is also notice from these figures that increase in inverse Darcy number $\left(Da^{-1}\right)$ leads to depreciates tangential skin friction coefficient and Nusselt number while enhance circumferential skin friction coefficient and Sherwood number. Increasing thermophoretic parameter (k) leads to rise in tangential and circumferential skin friction coefficients and Nusselt number while depreciation in Sherwood number is also noticed from these figures.

Figures 16 – 19 illustrates the variation of Forchheimer parameter (Γ) and ratio of angular velocities (λ) on tangential and circumferential skin friction coefficients, Nusselt number and Sherwood numbers. As Forchheimer parameter increases, tangential skin friction coefficients, Nusselt number and Sherwood number results decreased but circumferential skin friction coefficients increases. It is also noticed from these figures that increase in ratio of angular velocities causes to enhance tangential and circumferential skin friction coefficients but Nusselt number and Sherwood number results are reduced considerably.

Figures 20-22 depicts the wall thermophoretic deposition velocity (V_{tw}) for different values of relative temperature parameter, Forchheimer parameter and ratio of angular velocities. Fig. 20 reveals that increase in relative temperature parameter retards the wall thermophoretic velocity. From fig. 21 it is seen that wall thermophoretic velocity increases with increasing values of Forchheimer parameter. As increase in ratio of angular velocities, wall thermophoretic velocity increases as shown in fig. 22. It is also mentioned from figures 20-22 that increase in thermophoretic coefficient decreases wall thermophoretic velocity.

ISSN: 2277-9655
(I2OR), Publication Impact Factor: 3.785
(ISRA), Journal Impact Factor: 2.114

Table-1: The values of $-H''(0), -G'(0)$ ***and*** $-\theta'(0)$ ***for different values of Pr for*** $g_s = \frac{Gr}{\mathrm{Re}^2} = 0.1$ $Da^{-1} = 0$, Γ ***=0,*** $\lambda = 1$***, and*** $N = 0$ ***(in the absence of concentration equation).***

Pr	$-H''(0)$		$-G'(0)$		$-\theta'(0)$	
	Himasekhar et.al [15]	**Present work**	**Himasekhar et.al [15]**	**Present work**	**Himasekhar et.al [15]**	**Present work**
1.0	1.1282	1.12824	0.6437	0.64374	0.5457	0.54573
2.0	1.1120	1.11203	0.6335	0.63347	0.7450	0.74502
10	1.0702	1.07018	0.6202	0.62021	1.4106	1.41066

CONCLUSION

In this paper, the effect of Thermophoresis on double diffusive mixed convective heat and mass transfer flow of a Newtonian rotating fluid past a rotating vertical cone in a non-Darcy porous medium has been analyzed numerically. The study leads to the following conclusions:

1. Increasing Forchheimer parameter enhances circumferential and normal velocity, temperature and concentration profiles and circumferential skin friction coefficient but depreciates tangential velocity and tangential skin friction coefficient, Nusselt number and Sherwood number.
2. As increase in ratio of angular velocities, tangential velocity profile, Nusselt number and Sherwood number decreases but circumferential and normal velocity, temperature and concentration profiles, tangential and circumferential skin friction coefficients are enhanced.
3. Increase in relative temperature parameter and thermophoretic coefficients leads to enhancement of tangential and circumferential skin friction coefficients and Nusselt number while Sherwood reported opposite results.
4. Increasing inverse Darcy number leads to depreciates tangential skin friction coefficient and Nusselt number while accelerates circumferential skin friction coefficient and Sherwood number.

REFERENCES

[1] A.D. Nield, and A, Bejan, Convection in porous media, (2006), 3rd edn. Springer, New York.
[2] D.B. Ingham, and I. Pop, Transport phenomena in porous media, Pergamon, Oxford, vol II, 2002.
[3] Vafai K, Handbook of porous media, 2nd edn. (2005), Taylor & Francis, New York
[4] Bejan A, Dincer I, Lorente S, Miguel AF, Reis AH (2004) Porous and complex flow structures in modern technologies. Springer, New York
[5] K. Das, Effect of chemical reaction and thermal radiation on heat and mass transfer flow of MHD micropolar fluid in a rotating frame of reference, International Journal of Heat and Mass Transfer, 54, (2011), 3505-3513.
[6] M. Schuler, H.M. Dreher, S.O. Neumann, B. Weigand, and M. Elfert, Numerical predictions of the effect of rotation on fluid flow and heat transfer in an engine similar two pass internal cooling channel with smooth and ribbed walls, ASME Journal of Turbomachinery, 134, (2012), 021021-1-10.
[7] M.M. Rashidi, S. Abelman, N. Freidooni Mehr, Entropy generation in steady MHD flow due to a rotating porous disk in a nanofluid, International Journal of Heat and Mass Transfer, 62, (2013), 515-525.
[8] R. Bhuvanavijaya and B. Mallikarjuna, Effect of variable thermal conductivity on convective heat and mass transfer over a vertical plate in a rotating system with variable porosity regime, International Journal of Naval Architecture and Marine Engineering, 11, (2014), 83-92.
[9] P.V. Satyanarayana, B. Venkateswarlu, and S. Venkataramana, Thermal radiation and heat source effects on a MHD nanofluid past a vertical plate in a rotating system with porous medium, Heat Transfer – Asian Research, 44(1), (2015), 1-19.

ISSN: 2277-9655
(I2OR), Publication Impact Factor: 3.785
(ISRA), Journal Impact Factor: 2.114

[10] S. Saravanan, Centrifugal acceleration induced convection in a Magnetic fluid saturated anisotropic rotating porous medium, Transport in Porous Medium, 77, (2009), 79-86.
[11] A.J. Chamkha and S.E. Ahmed, unsteady MHD heat and mass transfer by mixed convection flow in the forward stagnation region of a rotating sphere at different wall conditions, Chemical engineering in communications, 199, (2012), 122-141.
[12] S. Nadeem and S. Saleem, Analytical study of rotating non-Newtonian nanofluid on a rotating cone, Journal of Thermophysics and Heat Transfer, 28(2), (2014), 295-302.
[13] S. Hariprasad Raju, B. Mallikarjuna and S.V.K.Varma, Thermophoretic effect on double diffusive convective flow of a chemically reacting fluid over a rotating cone in porous medium, International Journal of Scientific and Engineering Research, 6(1), (2015), 198-204.
[14] D. Srinivasacharya, B. Mallikarjuna and R. Bhuvanavijaya, Soret and Dufour effects on mixed convection along a vertical wavy surface in a porous medium with variable properties, Ain Shams Engineering Journal, Article in Press, 2015.
[15] K. Himasekhar, P.K. Sarma and K. Janardhan, Laminar mixed convection from a vertical rotating cone, International Communication in Heat and Mass Transfer, 16, 1989, 99-106.

GRAPHS

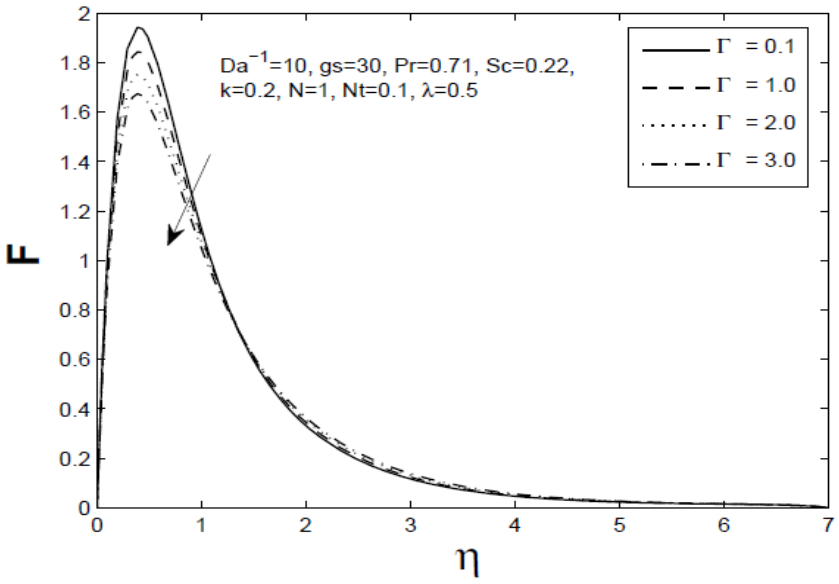

Fig 2: Tangential Velocity profile (F) ***for different values of Forchheimer parameter*** (Γ)

ISSN: 2277-9655
(I2OR), Publication Impact Factor: 3.785
(ISRA), Journal Impact Factor: 2.114

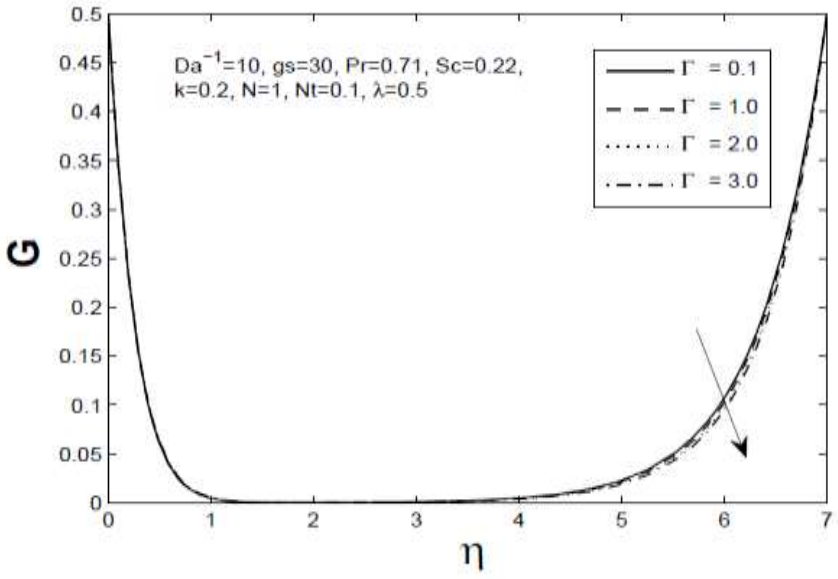

Fig 3: Circumferential Velocity profile (G) *for different values of Forchheimer parameter* (Γ)

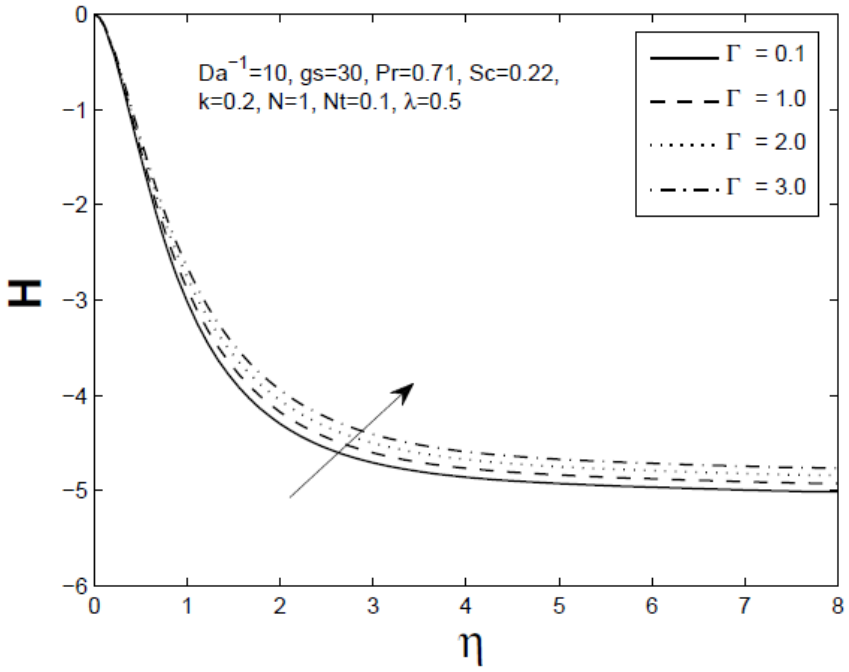

Fig 4: Normal Velocity profile (H) *for different values of Forchheimer parameter* (Γ)

ISSN: 2277-9655
(I2OR), Publication Impact Factor: 3.785
(ISRA), Journal Impact Factor: 2.114

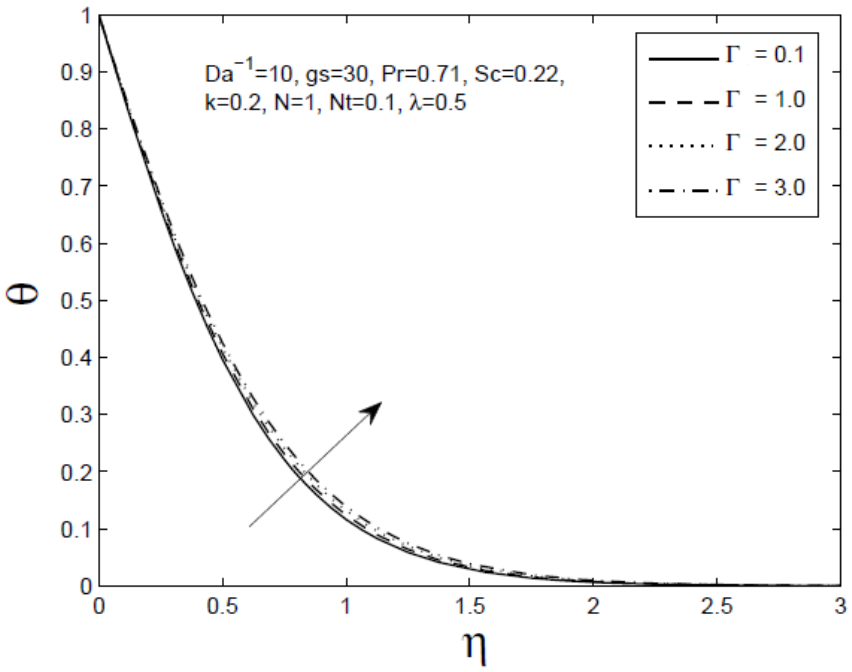

Fig 5: Temperature profile (θ) for different values of Forchheimer parameter (Γ)

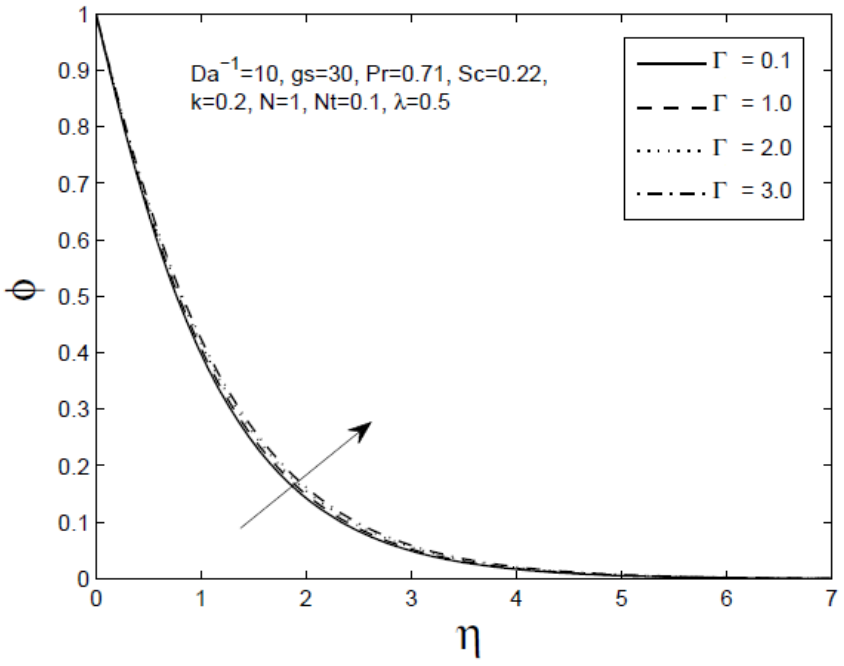

Fig 6: Concentration profile (ϕ) for different values of Forchheimer parameter (Γ)

ISSN: 2277-9655
(I2OR), Publication Impact Factor: 3.785
(ISRA), Journal Impact Factor: 2.114

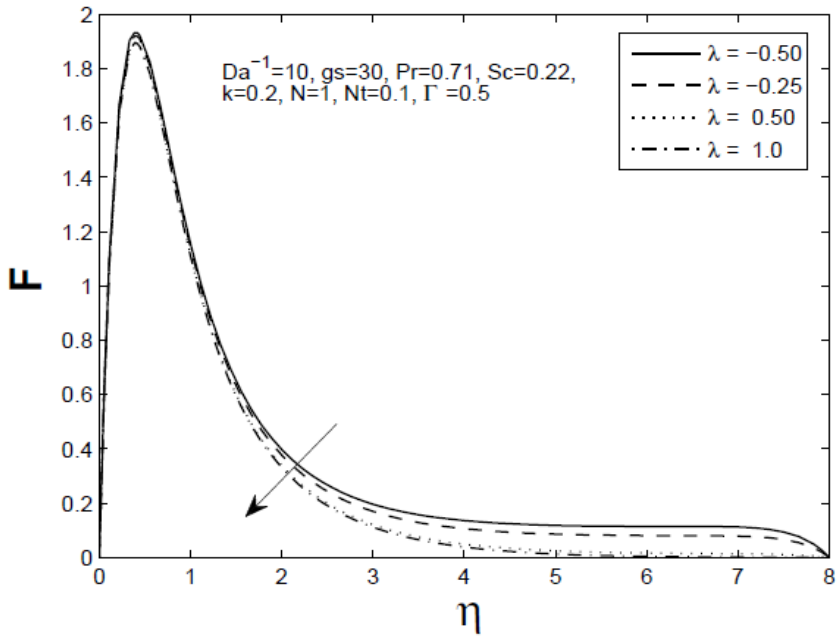

Fig 7: Tangential Velocity profile (F) *for different values of ratio of angular velocities* (λ)

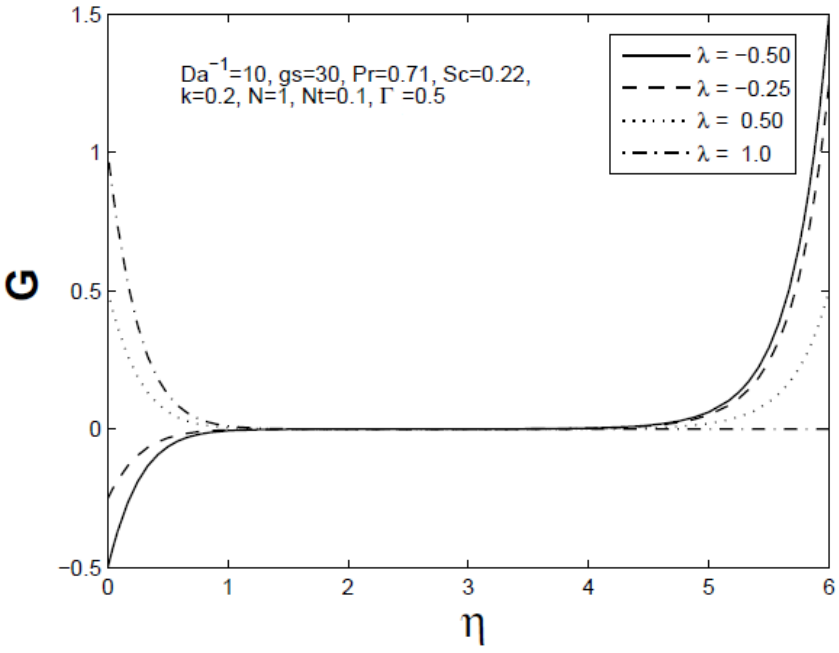

Fig 8: Circumferential Velocity profile (G) *for different values of ratio of angular velocities* (λ)

ISSN: 2277-9655
(I2OR), Publication Impact Factor: 3.785
(ISRA), Journal Impact Factor: 2.114

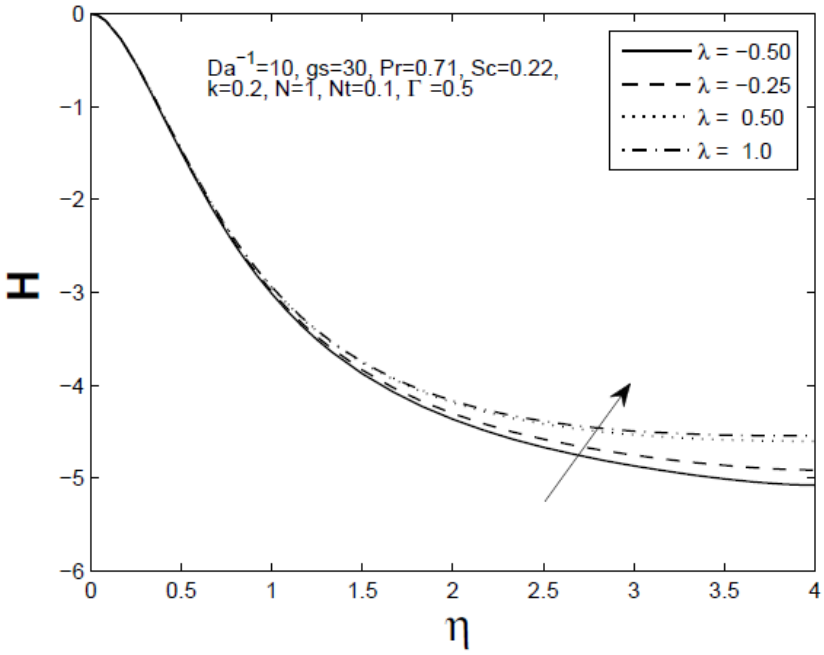

Fig 9: Normal Velocity profile (H) *for different values of ratio of angular velocities* (λ)

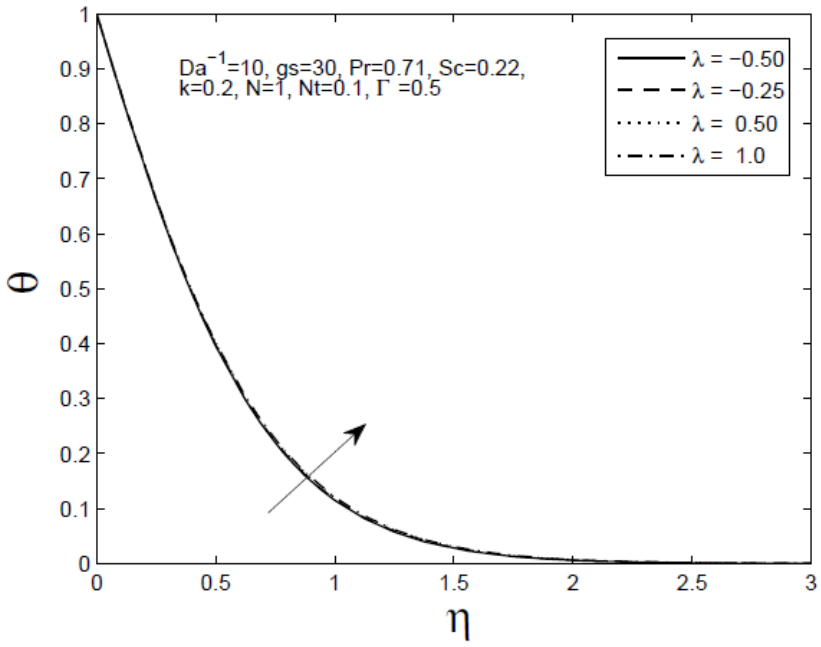

Fig 10: Temperature profile (θ) *for different values of ratio of angular velocities* (λ)

ISSN: 2277-9655
(I2OR), Publication Impact Factor: 3.785
(ISRA), Journal Impact Factor: 2.114

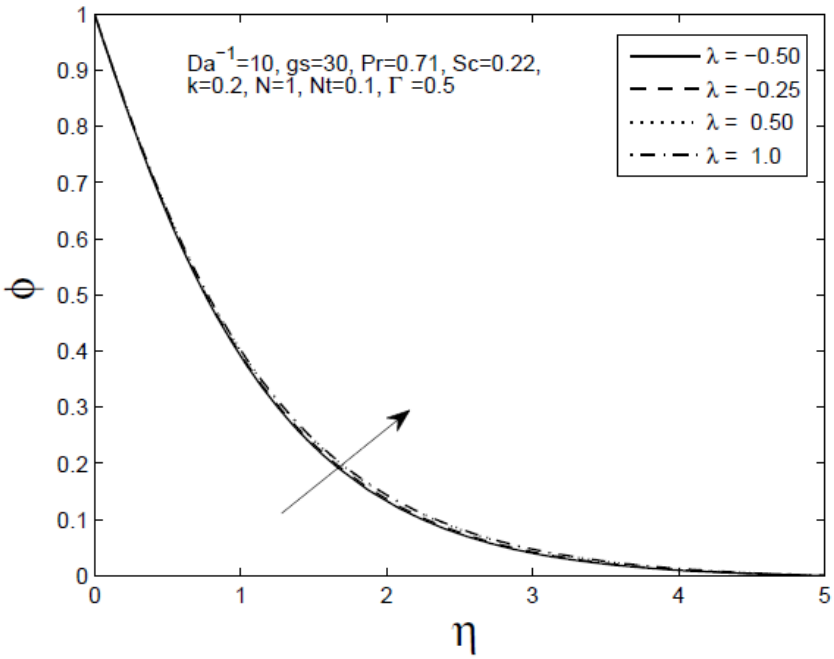

Fig 11: Concentration profile (ϕ) *for different values of ratio of angular velocities* (λ)

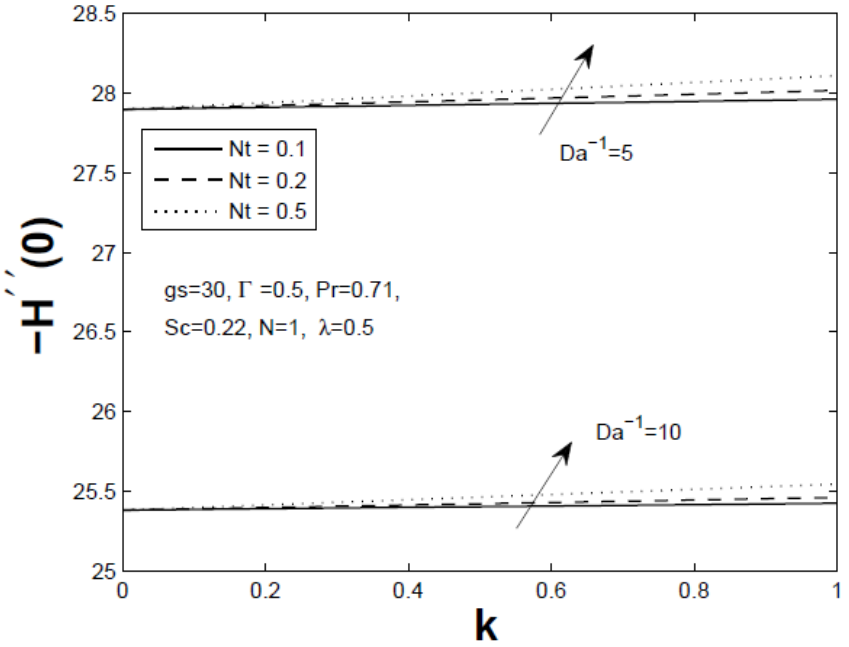

Fig 12: Tangential skin-friction co-efficient $(-H''(0))$ *for different values of inverse Darcy parameter* (Da^{-1}) *and relative temperature parameter* (Nt)

ISSN: 2277-9655
(I2OR), Publication Impact Factor: 3.785
(ISRA), Journal Impact Factor: 2.114

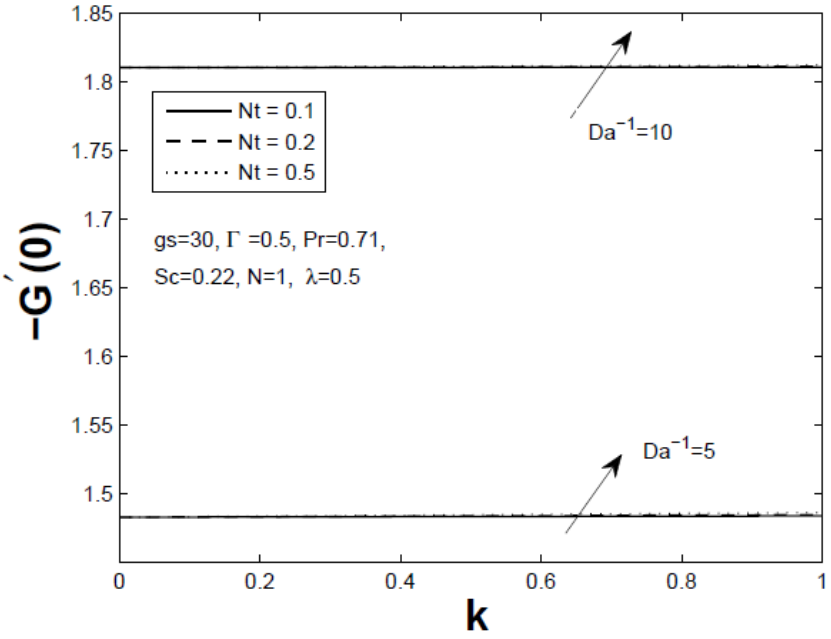

Fig 13: Azimuthal skin-friction co-efficient $(-G'(0))$ ***for different values of inverse Darcy parameter*** (Da^{-1}) ***and relative temperature parameter*** (Nt)

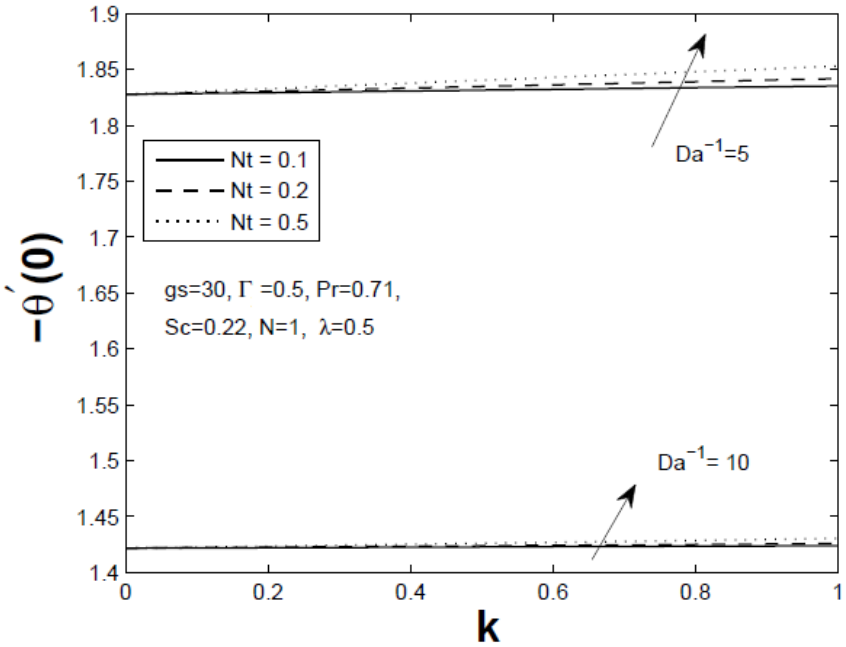

Fig 14: Local Nusselt number $(-\theta'(0))$ ***for different values of inverse Darcy parameter*** (Da^{-1}) ***and relative temperature parameter*** (Nt)

ISSN: 2277-9655
(I2OR), Publication Impact Factor: 3.785
(ISRA), Journal Impact Factor: 2.114

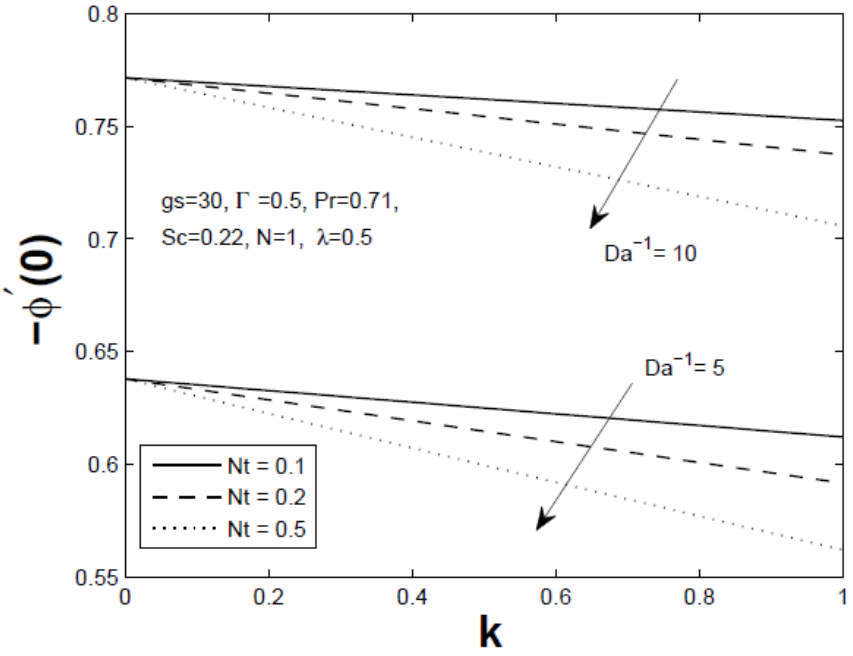

Fig 15: Local Sherwood number $(-\phi'(0))$ ***for different values of inverse Darcy parameter*** (Da^{-1}) ***and relative temperature parameter*** (Nt)

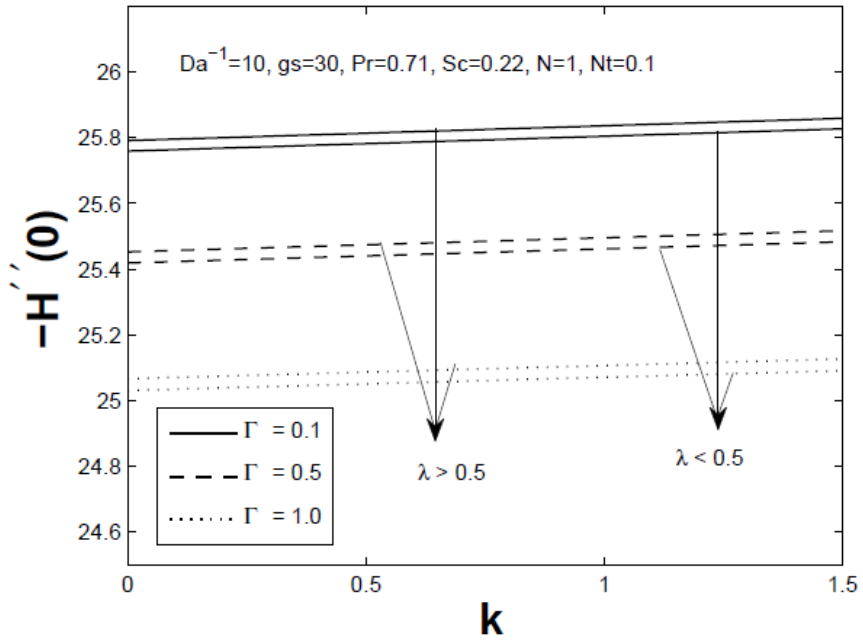

Fig 16: Tangential skin-friction co-efficient $(-H''(0))$ ***for different values of Forchheimer parameter*** (Γ) ***and ratio of angular velocities*** (λ)

ISSN: 2277-9655
(I2OR), Publication Impact Factor: 3.785
(ISRA), Journal Impact Factor: 2.114

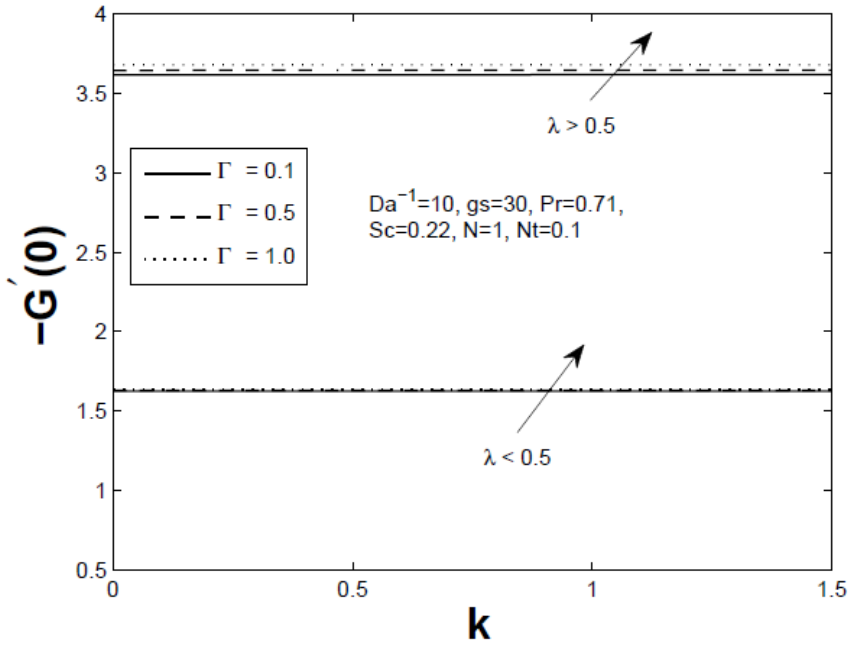

Fig 17: Azimuthal skin-friction co-efficient $(-G'(0))$ ***for different values of Forchheimer parameter*** (Γ) ***and ratio of angular velocities*** (λ)

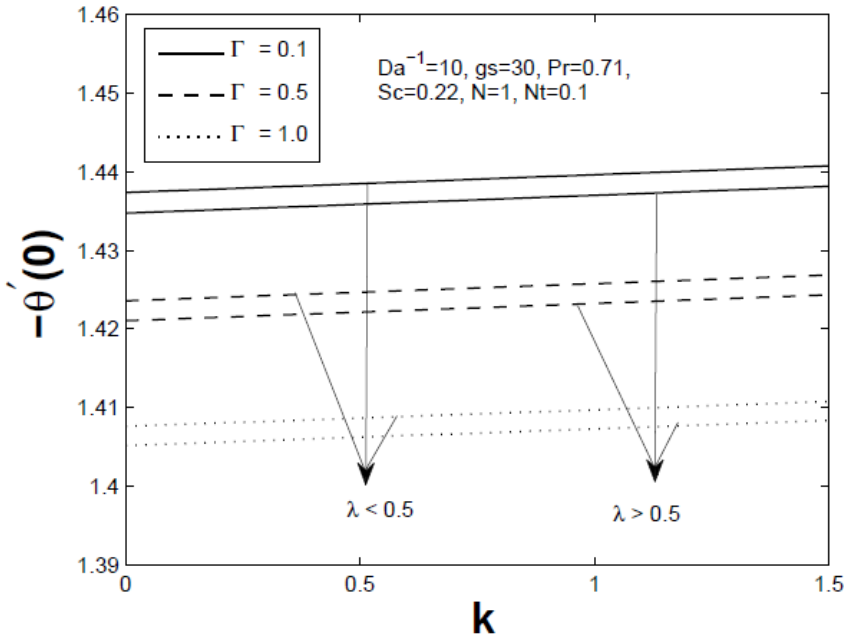

Fig 18: Local Nusselt number $(-\theta'(0))$ ***for different values of Forchheimer parameter*** (Γ) ***and ratio of angular velocities*** (λ)

ISSN: 2277-9655
(I2OR), Publication Impact Factor: 3.785
(ISRA), Journal Impact Factor: 2.114

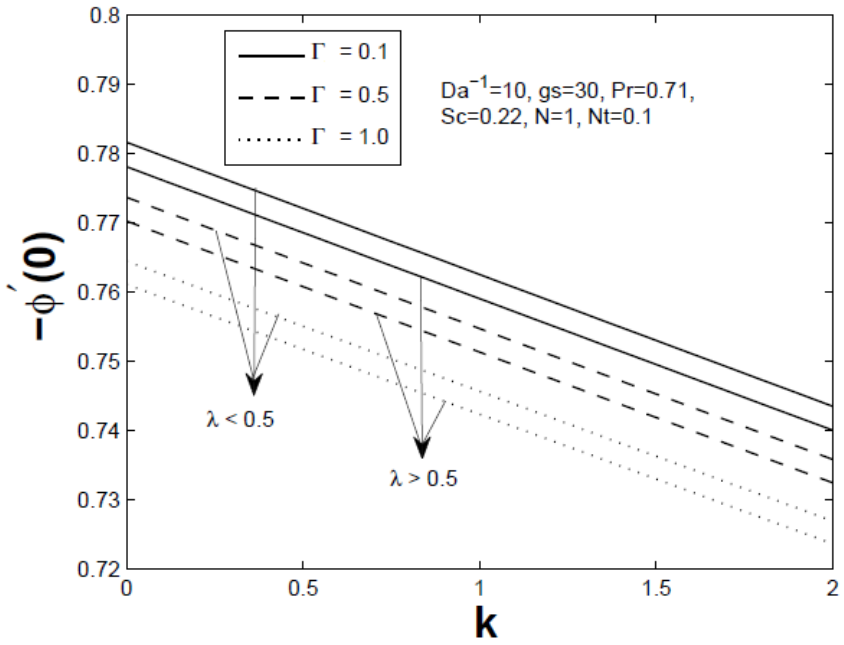

Fig 19: Local Sherwood number $(-\phi'(0))$ *for different values of Forchheimer parameter* (Γ) *and ratio of angular velocities* (λ)

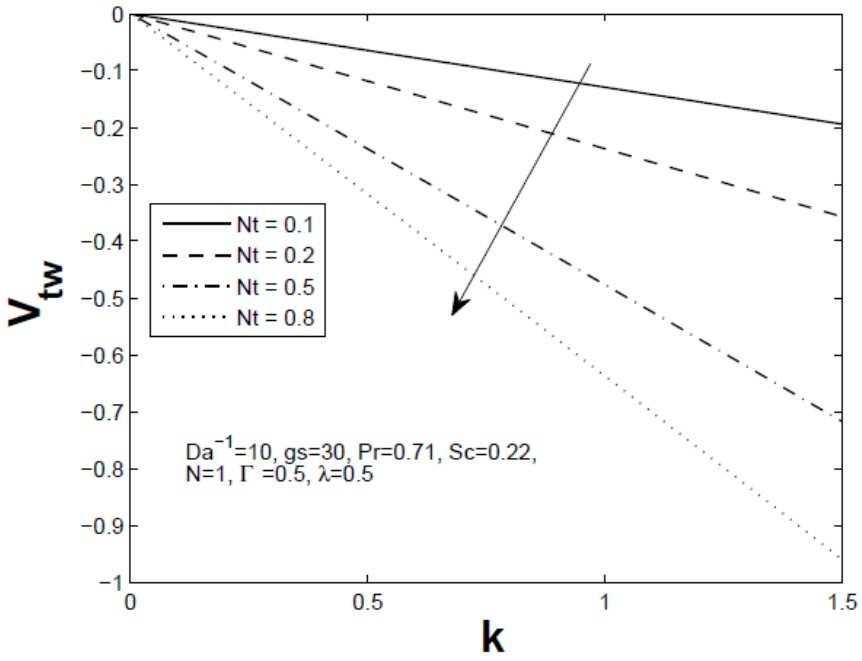

Fig 20: Wall temperature velocity (V_{tw}) *for different values of relative temperature parameter* (Nt)

ISSN: 2277-9655
(I2OR), Publication Impact Factor: 3.785
(ISRA), Journal Impact Factor: 2.114

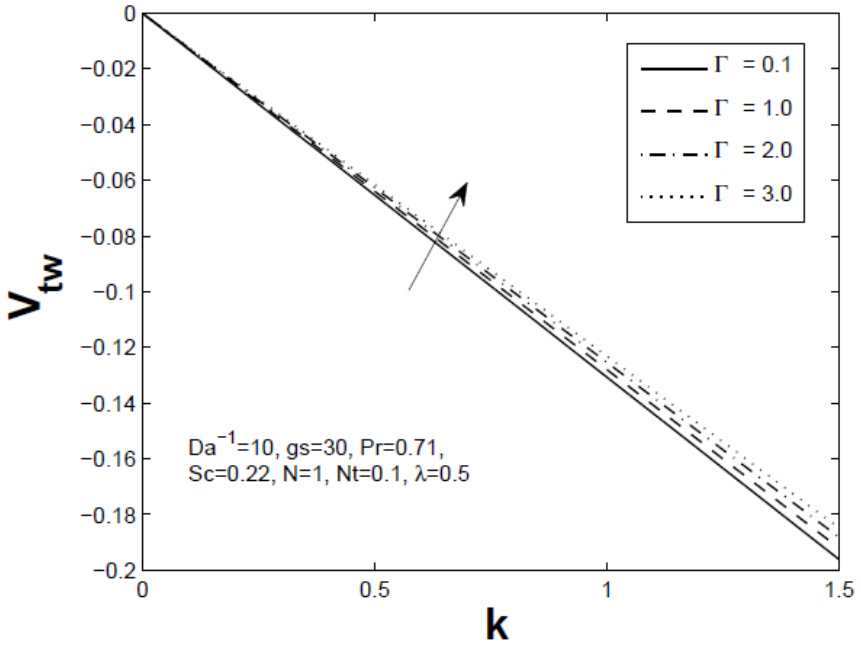

Fig 21: Wall temperature velocity (V_{tw}) *for different values of Forchheimer parameter* (Γ)

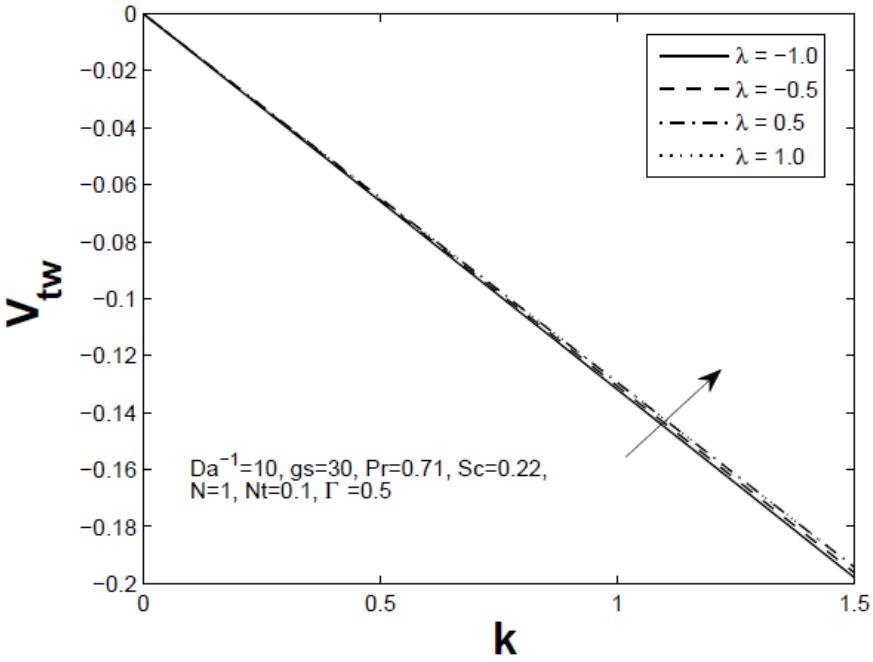

Fig 22: Wall temperature velocity (V_{tw}) *for different values of ratio of angular velocities* (λ)